Application of Lewis analogy to estimate the heat and mass transfer in membrane distillation

Wladyslaw Kaminski*, Elwira Tomczak, Bartosz Opara, Michal Tylman

Lodz University of Technology, Faculty of Process and Environmental Engineering, Wolczanska 213, 90-924 Lodz, Poland, email: wladyslaw.kaminski@p.lodz.pl (W. Kaminski)

a b s t r a c t

Desalination of the saltwater is an important technological process used to obtain not only drinking water but also to treat wastewater, for example, from dyes, textile, and mining industries. Methods based on evaporation of the solvent in multi-section evaporators or flesh evaporation are used for the desalination of water and wastewater. However, the most common methods applied in this process such as reverse osmosis, pervaporation, electrodialysis, and membrane distillation are based on membranes. The latter has gained great popularity in recent years. The heat obtained from renewable energy sources or waste heat can be used to perform this kind of process. The use of such heat sources significantly reduces the operating costs of the process, which directly determines the price of the obtained water. This work was carried out to study the membrane distillation process using a flat polysulfone ultrafiltration membrane PS35 (Sepro, USA) for various feed temperature (40°C–65°C) and water salinity (8‰–35‰). The results of the experiments were compared with simulated calculations. The simulation-based on the "section in series" model was carried out using MATLAB. The main assumption in the simulation was to adopt the Lewis analogy linking the heat transfer coefficient with the mass transfer coefficient which allows the amount of water vapor mass flux assessment. Verification and validation of the model for the laboratory scale showed the adequacy of the assumptions and a good match of the results obtained from experiments and calculations.

Keywords: Saline water; Polysulfone membrane; Computer simulation

1. Introduction

Over one billion people in the world do not have access to drinkable water. This problem occurs especially in desert regions with very low or even zero annual rainfall. There is, therefore, a great need to purify water unsuitable for human use such as seawater to obtain potable water. One of the methods of water desalination is the membrane distillation (MD) process. This method can desalinate water at lower temperatures than conventional distillation and much lower pressures than reverse osmosis, so MD has great potential to reduce energy consumption in the desalination process [1].

Membrane distillation can be carried out in several different variants, they differ from each other in the vapor condensation method [2,3].

1.1. Direct contact membrane distillation

In this variant, the membrane is in direct contact with the liquid phases on both sides. Permeate condenses directly on the membrane and is mixed with previously cooled permeate. This is the simplest configuration that can provide a reasonable permeate flux, which is why it is most common in laboratory-scale research. Its disadvantage is low energy efficiency in comparison with other variants.

* Corresponding author.

The reason for this is the direct contact of the membrane with the liquid on both sides. It is suitable for applications such as desalination or concentrating aqueous solutions, for example, to make concentrated juices.

1.2. Vacuum membrane distillation

It is characterized by the fact that on the permeate side there is steam or air under reduced pressure. Permeate is removed from the contactor in a gaseous form and condenses later in a separate device. This variant of membrane distillation is useful when volatile components are removed from aqueous solutions.

1.3. Sweep gas membrane distillation

In this configuration, cold stripping gas is used as a carrier for permeate vapors passing through the membrane. In this variant, condensation also takes place in a separate device other than the membrane contactor. This configuration is the least common of the four basic variants due to the costs of an additional external permeate condensation system. Like the vacuum membrane distillation, this variant is used to remove volatile components from aqueous solutions.

1.4. Air gap membrane distillation

In this type of contactor, permeate condensation occurs on the cooling plate, which forms a closed chamber on the cold side of the contactor. This construction method ensures the highest energy efficiency, however, the permeate stream obtained is usually quite small, which means that the membrane surface must be larger than in other variants. The air gap contactor configuration can be used in most applications of the membrane distillation process, especially in situations where energy availability is limited.

In recent years, a considerable amount of research in this field has been conducted, including mathematical simulations.

The simulation of MD processes can be carried out using models of various sizes: zero-dimensional (0-D), one-dimensional (1-D), and two-dimensional (2-D). The zero-dimensional models are models that don't analyze changes in the properties of the liquid in the way of their flow along the membrane. This means that this type of model doesn't take into account changes in temperature along with the module and hence also changes in the driving force of the process.

For this reason, they don't allow easy to change the scale [4,5]. The 1-D models are among the least used models. The model of this type takes into account changes in parameters such as temperature and salinity of the liquid along the membrane. They allow simulating the MD process regardless of the scale of the module, and the type of flow (co-current or counter-current) [6,7]. The 2-D models usually utilized computational fluid dynamic simulations computational fluid dynamics of flow parameters and heat transfer through a two-dimensional membrane [8].

In this paper 2-D model for AGMD in co-current flow regimes and the flat module was developed. Calculations were performed using our program coded in MATLAB. The theoretical model was compared with experimental data obtained for the PS35 membrane and feed temperatures in the range from 40°C to 70°C.

2. Model development

The paper presents a mathematical model of the membrane distillation process in AGMD configuration that worked with a flat membrane.

For the simulation of the process was used "section in the series" model. The laboratory membrane module was divided into assumed series of sections. The mathematical model was simplified according to the following assumptions:

- no membrane wetting takes place;
- membrane module works at steady-state conditions;
- there is no heat loss into the surrounding environment;
- heat resistances of condensate film (small thickness) and cooling plate (high thermal conductivity) are negligibly small;
- only water vapor is transported through the membrane;

Fig. 1 shows the temperature profile in a membrane module operating in AGMD configuration.

Most models of MD use a semi-empirical approach describing water vapor mass flux based on the difference of saturated vapor pressure on the feed side $p_{\text{feed}}^{\text{sat}}$ and on the permeate side $p_{\text{per}}^{\text{sat}}$.

The proportionality coefficient ϕ_m called the permeation coefficient depends on the microstructural properties of the membrane, such as porosity, pore tortuosity, and pore size. This coefficient ϕ_m was determined based on experimental data.

$$J_W = \phi_m \cdot \left(p_{\text{feed}}^{\text{sat}} - p_{\text{per}}^{\text{sat}} \right) \tag{1}$$

where J_W is the water mass flux (kg/(m² s)), ϕ_m is the membrane water permeation coefficient (kg/(m² Pa·s)), $p_{\text{feed}}^{\text{sat}}$ and $p_{\text{per}}^{\text{sat}}$ are the are saturated vapor pressure on the feed and permeate side [9].

The basis of the presented model is the mass and heat balance taking into account heat transport, mass transfer, and latent heat. Temperature change in the time corresponds with the amount of heat transferred from the saline feed to the coolant increased by the vapor condensation heat resulting from mass transport. Eq. (2) presents the above balance.

$$A \cdot K \cdot \left(T_{\text{feed},i} - T_{\text{cw},i} \right) + A \cdot K_{Y,i} \left[Y\left(T_{\text{mag},i} \right) - Y\left(T_{\text{cf},i} \right) \right] \cdot$$
$$r = W_{\text{cw}} \cdot C_{\text{cw}} \cdot \left(T_{\text{cw},i} - T_{\text{cw},i-1} \right) \tag{2}$$

where A is the surface area of slice i (m²), K is the overall heat transfer coefficient for membrane module (W/(m² K)), $K_{Y,i}$ is the mass transfer coefficient (kg/(m² s)), r is the latent heat of evaporation (J/kg), W_{cw} is the mass flow of cooling water (kg/s), C_{cw} is the specific heat of cooling water (J/(kg K)), $Y(T_{\text{mag},i})$ is the relative humidity at a temperature of the membrane surface facing the air channel (kg/kg), $Y(T_{\text{cf},i})$ is the relative humidity in temperature of
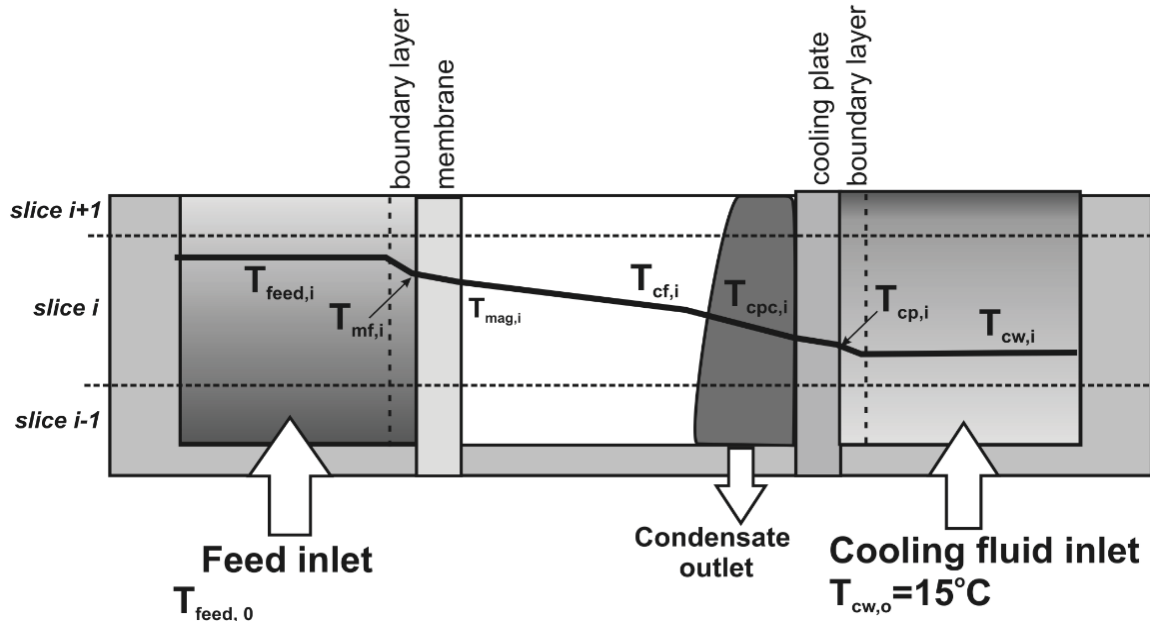
Fig. 1. The temperature profile in the AGMD module.

condensing film (kg/kg), $T_{feed,i}$, $T_{cw,i}$ is the temperatures of feed and cooling water in slice i, $T_{cw,i-1}$ is the temperature of cooling water in the preceding slice.

The calculations start with the assumption of constant feed temperature and a constant temperature of the cooling medium. These temperatures are changing during numerical calculations. The next calculation step is to determine the thermal resistance of the membrane contactor elements from Eq. (3).

$$R = \frac{1}{\alpha_1} + \frac{\delta_{mem}}{\lambda_{mem}} + \frac{\delta_{gap}}{\lambda_{gap}} + \frac{1}{\alpha_{con}} + \frac{\delta_{cp}}{\lambda_{cp}} + \frac{1}{\alpha_2} \tag{3}$$

where α_1, α_2 is the heat transfer coefficient of the MD feed and of the cooling water side boundary layer (W/(m² K)), δ_{mem}, δ_{gap}, δ_{cp} is the thickness of the membrane, air gap and cooling plate (m), λ_{mem}, λ_{gap}, λ_{cp} is the thermal conductivity of membrane, air gap, cooling plate (W/(m K)), α_{con} is the heat transfer coefficient of the condensate film (W/(m² K)).

As a result of the preliminary calculations, it was found that the elements $\frac{1}{\alpha_{con}}, \frac{\delta_{cp}}{\lambda_{cp}}$ of the equation can be considered negligibly small. Thermal conductivity of the membrane λ_{mem} is evaluated based on the following equation:

$$\lambda_{mem} = \varepsilon \cdot \lambda_{avm} + (1-\varepsilon)\lambda_{poly} \tag{4}$$

where ε is the membrane porosity (–), λ_{avm} is the thermal conductivity of air and water vapor mixture and λ_{poly} is the thermal conductivity of polymer (W/(m K)).

Heat transfer coefficients of the boundary layer α_1 and α_2 can be described by the Nusselt correlation, where Nusselt number is a function of Reynolds and Prandtl numbers [8].

For laminar flow (Re < 2,100):

$$Nu = 0.664 \cdot Pr^{0.33} \cdot Re^{0.5} \tag{5}$$

For turbulent flow (Re > 10⁴):

$$Nu = 0.23 \cdot Pr^{0.4} \cdot Re^{0.8} \tag{6}$$

Nusselt number:

$$Nu = \frac{\alpha \cdot d}{\lambda} \tag{7}$$

Reynolds number:

$$Re = \frac{v \cdot d \cdot \rho}{\mu} \tag{8}$$

Prandtl number:

$$Pr = \frac{C_F \cdot \mu}{\lambda} \tag{9}$$

where v, ρ, μ, C_F, λ, d is the fluid velocity (m/s), density (kg/m³), viscosity (Pa·s), specific heat (J/(kg K)), thermal conductivity (W/(m K)), characteristic diameter (m), respectively.

Thermal resistance for the module allows to determine the overall heat transfer coefficient K for the module from the formula:

$$K = \frac{1}{R} \tag{10}$$

The amount of exchanged heat by convection and conduction is described by Eq. (11):

$$Q_i = A \cdot K \cdot \left(T_{\text{feed},i} - T_{\text{cw},i} \right) \tag{11}$$

where Q_i is the overall heat transfer in slice i (W).

Taking into account that the process takes place under steady conditions, appropriate temperatures can be determined in each slice according to Eqs. (12)–(14).

$$T_{\text{mf},i} = T_{\text{feed},i} - \frac{Q_i}{\alpha_1 \cdot A} \tag{12}$$

$$T_{\text{mag},i} = T_{\text{mf},i} - \frac{Q_i \cdot \delta_{\text{mem}}}{\lambda_{\text{mem}} \cdot A} \tag{13}$$

$$T_{\text{cp},i} = T_{\text{mag},i} - \frac{Q_i \cdot \delta_{\text{gap}}}{\lambda_{\text{gap}} \cdot A} \tag{14}$$

where $T_{\text{mf},i}$, $T_{\text{mag},i}$, $T_{\text{cp},i}$ is the temperatures (°C): membrane from the feed side, the membrane of air gap side, a cooling plate from the cooling waterside.

The second part of the balance defines the amount of heat that is released during the condensation of the water vapor. The mass transfer coefficient $K_{Y,i}$ in the membrane distillation process can be calculated by analogy with liquid evaporation processes. Numerous research works have shown that the ratio of the heat transfer coefficient to the mass transfer coefficient can be expressed by the equation known as the Lewis analogy:

$$\frac{\alpha}{K_{Y,i}} = C_H \tag{15}$$

where C_H is humid specific heat which can be written as:

$$C_H = C_{\text{da}} + Y \cdot C_{\text{wv}} \tag{16}$$

where C_{da}, C_{wv} is the specific heat of dry air and water vapor (J/(kg K)) and Y is humidity ratio (kg of water vapor/kg of dry air).

Condensate flux $Q_{c,i}$ (kg/s) for the i-th slice is expressed by the equation:

$$Q_c = A \cdot K_{Y,i} \times \left(Y\left(T_{\text{mag},i} \right) - Y\left(T_{\text{cf},i} \right) \right) \tag{17}$$

For which the relative humidity is determined using the following equations:

$$Y\left(T_{\text{mag},i} \right) = 0.622 \cdot \frac{P_{\text{sat},T_{\text{mag},i}}}{P - P_{\text{sat},T_{\text{mag},i}}} \tag{18}$$

$$Y\left(T_{\text{cf},i} \right) = 0.622 \cdot \frac{P_{\text{sat},T_{\text{cf},i}}}{P - P_{\text{sat},T_{\text{cf},i}}} \tag{19}$$

where $P_{\text{sat},T_{m,i}}$ and $P_{\text{sat},T_{\text{cf},i}}$ are the vapor saturation pressures at temperatures $T_{m,i}$ and $T_{\text{cf},i}$.

The total condensate flux is calculated as the sum of the intensity of the permeate generation in each slice relative to the total surface of the membrane. The properties of seawater such as density, viscosity, thermal conductivity, saturation pressure were calculated according to the equations listed in Table 1. The algorithm allows us to calculate the total condensate flow generated in the module at given temperatures, feed and cooling water mass streams, and initial feed salinity. Two end conditions for the algorithm were adopted. The basic condition to terminate the algorithm is to meet the mass balance for the feed and permeate with an accuracy of 10^{-7}. Besides, a limited number of iterations was used. As a result of calculations for this calculation procedure, it was found that a sufficient number of iterations is 5.

3. Materials and method

3.1. Experimental setup and membranes

Commercially available polysulfone ultrafiltration membrane PS35 provided by Sepro (USA) was tested in the AGMD process. Membrane's pores diameter and contact angle were respectively 34 nm, 71.58°. The membrane of 10 cm × 10 cm was tested in a flat sheet module made of Acrylonitrile-Butadiene-Styrene (3D printing) and the cover was made from stainless steel.

The feed and cooling water channels were 10 mm in height. The condensate was collected on the bottom of the membrane module. Mass of condensate was measured on an electronic Mettler Toledo (Switzerland) balance, type XA105 DualRange.

The air gap width was 5 mm. Feed and cooling water temperatures were measured by PT100 sensors placed at the inlets. Feed temperature was controlled by a thermostatic heater. The schematic diagram of the experimental setup is shown in Fig. 2.
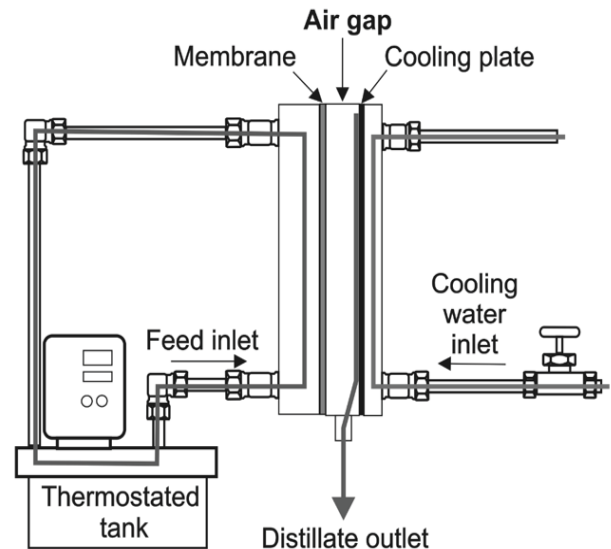

Fig. 2. Schematic diagram of the experimental setup.

Table 1
Seawater properties

Property	Equation	References
Thermal conductivity	$k_w = 0.797015 \cdot T^{-0.194} - 0.251242 \cdot T^{-4.717} + 0.096437 \cdot T^{-6.385} - 0.032696 \cdot T^{-2.134}$ T – dimensionless temperature given by $(t + 273.15)/300$ Validity: $0°C < t < 99°C$; pressure: 0.1 MPa	[10,11]
Latent heat of evaporation	$f_{fg,sw} = f_{fg,w} \cdot \left(1 - \dfrac{S}{1,000}\right)$ $f_{fg,sw}$ – latent heat seawater (J/K) $f_{fg,w}$ – latent heat of pure water (J/K) $f_{fg,w} = 2.501 \cdot 10^6 - 2.369 \cdot 10^3 \cdot t + 2.678 \cdot 10^{-1} \cdot t^2 - 8.103 \cdot 10^{-3} \cdot 3t^3 - 2.079 \cdot 10^{-5} \cdot t^4$ Validity: $0°C < t < 200°C$	[11]
Saturation (vapor) pressure of seawater	$\ln\left(\dfrac{p_{v,sw}}{p_{v,w}}\right) = -4.58180 \cdot 10^{-4} S - 2.04430 \cdot 10^{-6} S^2$ $p_{v,sw}$ – saturation pressure of seawater (Pa) $p_{v,w}$ – saturation pressure of pure water (Pa) S – salinity (g/kg) $\ln\left(p_{v,w}\right) = \dfrac{a_1}{t} + a_2 + \dfrac{a_3}{t} + \dfrac{a_4}{t^2} + \dfrac{a_5}{t^3} + a_6 \ln\left(t\right)$ $a_1 = -5,800$, $a_2 = 1.3915$, $a_3 = 4.8640 \cdot 10^{-2}$, $a_4 = 4.1765 \cdot 10^{-5}$, $a_5 = -1.4452 \cdot 10^{-8}$, $a_5 = 6.5460$ Validity: $0°C < t < 180°C$; 0 kg/kg $< S < 160$ g/kg	[10]

Specific heat at constant pressure	$C_{p,sw} = A + B(t + 273.15) + C(t + 273.15)^2 + D(t + 273.15)^3 + (P - 0.101325) \cdot$
	    $(a_1 + a_2 t + a_3 t^2 + a_4 t^3 + S \cdot (a_5 + a_6 t + a_7 t^2 + a_8 t^3))$
	$C_{p,sw}$ – specific heat at constant pressure of seawater (J/kg K)
	P – pressure (MPa)
	$A = 5,328 - 97.6 \cdot S + 4.04 \cdot 10^{-1} \cdot S^2$, $B = -6.913 + 7.351 \cdot 10^{-1} \cdot S + 3.15 \cdot 10^{-1} \cdot S^2$,
	    $C = 9.6 \cdot 10^{-3} - 1.927 \cdot 10^{-3} \cdot S + 8.23 \cdot 10^{-6} \cdot S^2$
	$a_1 = -3.1118$, $a_2 = 0.0157$, $a_3 = 5.1014 \cdot 10^{-5}$, $a_4 = -1.0302 \cdot 10^{-6}$, $a_5 = 0.0107$, $a_6 = -3.9716 \cdot 10^{-5}$,
	$a_7 = 3.2088 \cdot 10^{-8}$, $a_8 = 1.0119 \cdot 10^{-9}$
	Validity: $40 < t \leq 180°C$; $0 \leq S \leq 42$ g/kg; $0 \leq P \leq 12$ MPa
		[10,12]

Dynamic viscosity	$\mu_{sw} = \mu_w (1 + A \cdot S + B \cdot S^2)$ μ_{sw} – dynamic viscosity of seawater (Pa·s) μ_w – dynamic viscosity of pure water (Pa·s) $\mu_w = 4.2844 \cdot 10^{-5} + (0.157(t + 64.993)^2 - 91.296)^{-1}$ $A = 1.541 + 1.998 \cdot 10^{-2} \cdot t - 9.520 \cdot 10^{-5} \cdot t^2$ $B = 7.974 + 7.561 \cdot 10^{-2} \cdot t + 4.724 \cdot 10^{-4} \cdot t^2$ Validity: $0°C < t < 180°C$; 0 kg/kg $< S < 0.15$ kg	[11,13]

Table 2
Statistical evaluation of the experimental and the calculated data

Salinity (g/kg)	R^2 (–)	RMSE (kg/(m² h))
0	0.990	0.307
8	0.984	0.383
35	0.996	0.175

3.2. Experimental procedure

The air gap membrane distillation process was conducted for the feed with various salinity and temperature in the range of 40°C–70°C. The experiments were carried out for a feed with a salinity Sn_0 equal: 0 g/kg (control sample), 8 g/kg (average salinity of the Baltic Sea), 35 g/kg (Persian Gulf salinity). Each experiment lasted about 1 h and it was repeated three times to determine the
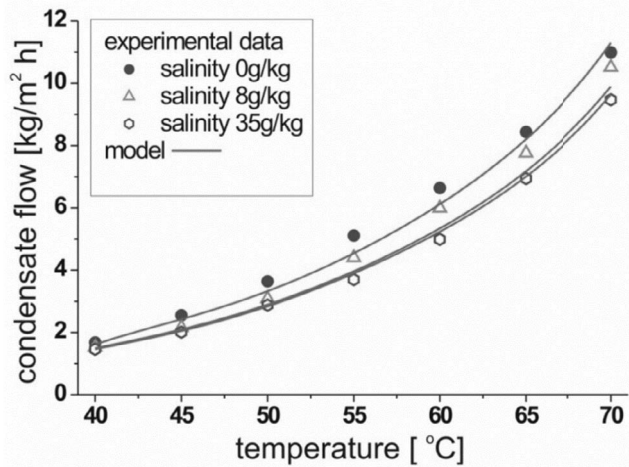
Fig. 3. Predicted and measured condensate flux for different salinity of feed.

standard deviation for the condensate flux. After each set, the membrane was washed with new feed. The membrane was not exchanging during all experiments.

The system contained about 3 L of feed liquid, in order to maintain a constant concentration of salt in the feed during the process collected permeate was returned to the feed liquid container. The feed flow rate was set to 17 L/min. In the refrigeration circuit, the water flow rate was around 5 L/min. Based on measurements of specific conductivity of salt solutions with concentrations respectively: 0, 8, 35, and the calibration curve was prepared to determine the salt concentration in the permeate.

During the experiment, the following process parameters were measured:

- permeate weight and time of obtaining it at a given temperature;
- specific conductivity of permeate;
- temperature of the feed and cooling water;

4. Results and discussion

Mathematical model results were validated with experimental data. Fig. 3 shows a comparison between simulated and measured fluxes of condensed vapor.

Table 2 provides a statistical evaluation of the experimental and calculated data. In the statistical evaluation, the following factors were taken into account the square of the determination coefficient (R^2) and the root of mean square error (RMSE).

The model allows us to simulate the process assuming only 4 input parameters, temperatures at the inlets, and mass flow rates (feed and cooling agent). The highest deviation of the simulation and the experimental data was observed for the salinity of 8 g/kg. For freshwater, the largest condensate flows are achieved.

The condensate flow decreases with increasing salinity. The highest condensate flow was observed for 70°C feed temperature. However, regardless of the process temperature,

the differences in permeate flow for different salinity were small.

Considering the salt concentration in the permeate, it should be stated that almost 100% desalination of the feed was achieved.

5. Conclusions

- AGMD model was developed based on the analogy of Lewis heat and mass transport.
- Good correlation between experimental results and calculated from the model was obtained.
- Air gap is the main resistance of heat transport and consequently mass transport. It should be as small as possible.
- An increase in the temperature in the feed causes a significant increase in the flow of permeates.
- Lewis analogy can be used in other types of membrane distillation.

Symbols

A	—	Surface area of slice i, m^2
C_{cw}	—	Specific heat of coolant water, J/(kg K)
C_H	—	Humid specific heat, J/kg K
$C_{p,sw}$	—	Specific heat at constant pressure of seawater, J/kg K
d	—	Characteristic diameter, m
$f_{fg,sw}$	—	Latent heat seawater, J/K
$f_{fg,w}$	—	Latent heat of pure water, J/K
J_W	—	Water mass flux, kg/s
K	—	Heat transfer coefficient for membrane module, W/(m^2 K)
$K_{Y,i}$	—	Mass transfer coefficient to condensate film, kg/(m^2 s)
Q_i	—	Heat exchanged through conduction in slice i in membrane module, W
$T_{cf,i}$	—	Temperatures of condensate at air gap side, °C
$T_{cpc,i}$	—	Temperatures of condensate at cooling plate side, °C
$T_{cw,i}$	—	Temperatures of cooling water in slice i, °C
$T_{cw,i-1}$	—	Temperature of cooling water in slice i–1, °C
$T_{feed,i}$	—	Temperatures of feed in slice i, °C
$T_{mf,i}$	—	Temperature of membrane from the feed side, °C
$T_{mag,i}$	—	Temperature of membrane of air gap side, °C
$T_{cp,i}$	—	Temperature of cooling plate from the cooling water side, °C
W_{cw}	—	Mass flow of coolant water, kg/s
C_p	—	Heat capacity, J/(kg K)
P	—	Pressure, MPa
p_{feed}^{sat}	—	Saturated vapor pressure on feed side, Pa
p_{per}^{sat}	—	Saturated vapor pressure on permeate side, Pa
$P_{sat,T_{m,i}}$	—	Vapor saturation pressures at temperatures $T_{m,i}$, Pa
$P_{sat,T_{cf,i}}$	—	Vapor saturation pressures at temperatures $T_{cf,i}$, Pa
$p_{v,sw}$	—	Saturation pressure of seawater, Pa
$p_{v,w}$	—	Saturation pressure of pure water, Pa
S	—	Salinity, g/kg

r	—	Latent heat of evaporation, J/kg
R	—	Thermal resistance of the membrane contactor, m^2K/W
V	—	Fluid velocity, m/s
$Y(T_{cf,i})$	—	Relative humidity in temperature of condensing film, K
$Y(T_{mag,i})$	—	Relative humidity in temperature at the surface of the membrane and facing the air channel, kg/kg
α_1	—	Heat transfer coefficient of the MD feed side boundary layer, $W/(m^2K)$
α_2	—	Heat transfer coefficient of the cooling water side boundary layer, $W/(m^2K)$
α_{con}	—	Heat transfer coefficient of the condensate film, $W/(m^2K)$
δ_{cp}	—	Thickness of the cooling plate, m
δ_{gap}	—	Thickness of the air gap, m
δ_{mem}	—	Thickness of the membrane, m
λ	—	Thermal conductivity, W/(m K)
λ_{cp}	—	Thermal conductivity of the cooling plate, W/(m K)
λ_{gap}	—	Thermal conductivity of the air gap, W/(m K)
λ_{mem}	—	Thermal conductivity of the membrane, W/(m K)
λ_{poly}	—	Thermal conductivity of polymer, W/(m K)
μ	—	Viscosity, Pa·s
μ_{sw}	—	Dynamic viscosity of seawater, Pa·s
μ_w	—	Dynamic viscosity of pure water, Pa·s
ρ	—	Density, kg/m^3
ε	—	Membrane porosity, –
ϕ_m	—	Membrane water permeation coefficient, $kg/(m^2\ Pa·s)$
Nu	—	Nusselt number, –
Re	—	Reynolds number, –
Pr	—	Prandtl number, –

References

[1] A. Alsaati, A.M. Marconnet, Energy efficient membrane distillation through localized heating, Desalination, 442 (2018) 99–107.

[2] L.M. Camacho, L. Dumée, J.H. Zhang, J.-D. Li, M. Duke, J. Gomez, S. Gray, Advances in membrane distillation for water desalination and purification applications, Water, 5 (2012) 94–196.

[3] P. Onsekizoglu, Chapter 11 – Membrane Distillation: Principle, Advances, Limitations and Future Prospects in Food Industry, S. Zereshki Ed., Distillation - Advances from Modeling to Applications, IntechOpen, 2012, doi: 10.5772/37625.

[4] H. Chang, C.-L. Chang, C.-D. Ho, C.-C. Li, P.-H. Wang, Experimental and simulation study of an air gap membrane distillation module with solar absorption function for desalination, Desal. Water Treat., 25 (2011) 251–258.

[5] F.A. Banat, J. Simandl, Desalination by membrane distillation: a parametric study, Sep. Sci. Technol., 33 (1998) 201–226.

[6] A.S. Alsaadi, N. Ghaffour, J.-D. Li, S. Gray, L. Francis, H. Maab, G.L. Amy, Modeling of air-gap membrane distillation process: a theoretical and experimental study, J. Membr. Sci., 445 (2013) 53–65.

[7] J.H. Zhang, S. Gray, J.-D. Li, Modelling heat and mass transfers in DCMD using compressible membranes, J. Membr. Sci., 387 (2012) 7–16.

[8] R. Chouikh, S. Bouguecha, M. Dhahbi, Modelling of a modified air gap distillation membrane for the desalination of seawater, Desalination, 181 (2005) 257–265.

[9] G.X. Dong, J.F. Kim, J.H. Kim, E. Drioli, Y.M. Lee, Open-source predictive simulators for scale-up of direct contact membrane distillation modules for seawater desalination, Desalination, 402 (2017) 72–87.

[10] K.G. Nayar, M.H. Sharqawy, L.D. Banchik, J.H. Lienhard V, Thermophysical properties of seawater: a review and new correlations that include pressure dependence, Desalination, 390 (2016) 1–24.

[11] M.H. Sharqawy, J.H. Lienhard V, S.M. Zubair, Thermophysical properties of seawater: a review of existing correlations and data, Desal. Water Treat., 16 (2010) 354–380.

[12] D.T. Jamieson, J.S. Tudhope, R. Morris, G. Cartwright, Physical properties of sea water solutions: heat capacity, Desalination, 7 (1969) 23–30.

[13] International Association for the Properties of Water and Steam, Release on the IAPWS Formulation 2008 for the Viscosity of Ordinary Water Substance, Berlin, 2008.